Generation of zero order Bessel beams with Fabry-Perot interferometer

Z. L. Horváth [a], M. Erdélyi [a], G. Szabó [a], Zs. Bor [a], F. K. Tittel [b] and J. R. Cavallaro [b]

[a] *Department of Optics and Quantum Electronics, JATE University, H-6701 P. O. Box 406, Szeged, Hungary*

[b] *Department of Electrical and Computer Engineering, Rice University, 6100 Main, Houston, TX 77005-1892, USA*

ABSTRACT

A new concept for generating zero order Bessel beams was studied. A point source illuminated a Fabry-Perot etalon, which produced a concentric interference ring system in front of an imaging lens. If the lens aperture was adjusted so that it transmitted the first ring only and blocked all others, a zero order Bessel beam was generated beyond the lens. The spatial intensity distribution beyond the lens was calculated numerically using a wave optical model. The calculated and measured axial intensity distributions were compared. An approximate analytical expression was derived to describe the radial intensity distribution in planes perpendicular to the optical axis.

Keywords: nondiffracting beams, Bessel beams, diffraction

1. INTRODUCTION

In 1987 Durnin showed[1] that the field given by $E(r,z,t)=A\,J_0(\alpha r)\exp[i(\beta z-\omega t)]$ is a solution of the wave equation, if $\alpha^2+\beta^2=\omega^2/c^2$, where $r^2=x^2+y^2$ and J_0 is the zero order Bessel function of the first kind (x, y, z are the Cartesian coordinates and c is the speed of light). An ideal zero order Bessel beam is made up of an equal–weight superposition of monochromatic plane waves with wave vectors lying in a conical surface having the same magnitude. There exist several experiments which achieve such a superposition of plane waves. This type of angular spectrum can be obtained by applying an annular slit (in the focal plane of a lens)[2], axicon[3], holographic process[4,5], Fabry-Perot interferometer[6,7] or new type of laser cavity[8,9].

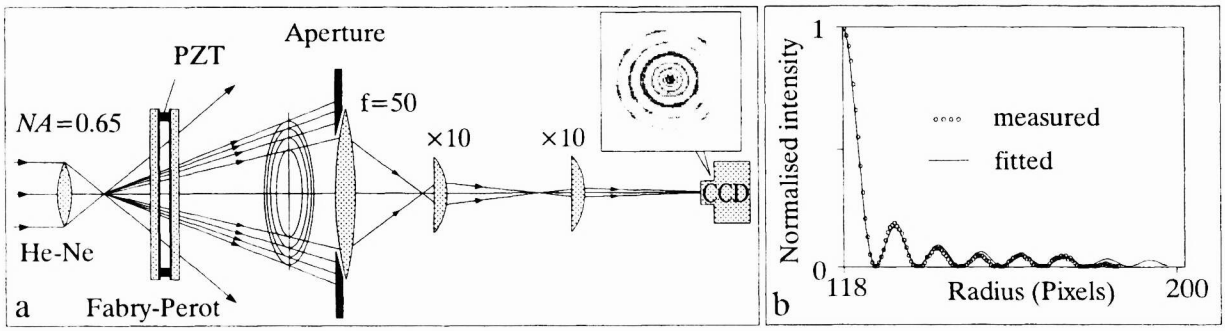

Fig. 1. a: Schematic diagram of the experimental setup for generating zero order Bessel beams. If the aperture is adjusted so that it transmits only the first Fabry–Perot ring, a zero order Bessel beam is generated beyond the lens. The image was magnified by two microscope objectives and observed with a CCD camera. **b:** The measured radial intensity distribution (circles) and the fitted curve given by the J_0 function in a plane perpendicular to the optical axis.

A new concept for the generation of nondiffracting Bessel beams was presented and proposed for microlithographic application in Ref. 10. The experimental arrangement is shown in Fig. 1a. A point like source was created by focusing the light of a He-Ne laser (λ=632.8 nm). This point source illuminated a scanning Fabry-Perot interferometer which produced

a concentric ring system in front of the lens. The aperture was adjusted so that it transmitted the first Fabry-Perot ring only and blocked all the others. The measured intensity distribution in planes being perpendicular to the optical axis is given by the J_0 function (Fig. 1b). This result was expected since the diffraction pattern of a narrow annular aperture can be described by the zero order Bessel function [11-13]. Due to the annular illumination of the lens the depth of focus increased and the transverse resolution can be improved [10] by a factor of 1.6.

2. THEORY

Suppose that a monochromatic spherical wave generated by a point source illuminates a Fabry-Perot interferometer and the light passing through the interferometer is incident on a thin lens with focal length f at wavelength λ (Fig. 2). Due to the multiple reflection in the interferometer the electric field in front of the lens is the same as the field generated by a sequence of point sources I_0, I_1, ... , I_m, ... as it is shown in Fig. 2. The distance between two neighboring sources is $2d$ and its intensity ratio is R^2 where d is the base of the etalon and R is the reflectivity of the mirrors. The radius q_m of the outgoing wave front immediately to the right of the lens is given by

$$1/q_m = 1/f - 1/p_m \quad , \tag{1}$$

where p_m is the radius of the incoming spherical wave front immediately to the left of the lens (Fig. 2). The electric behind the lens in point P can be calculated as the superposition of the fields produced by the virtual sources. It is given by [14]

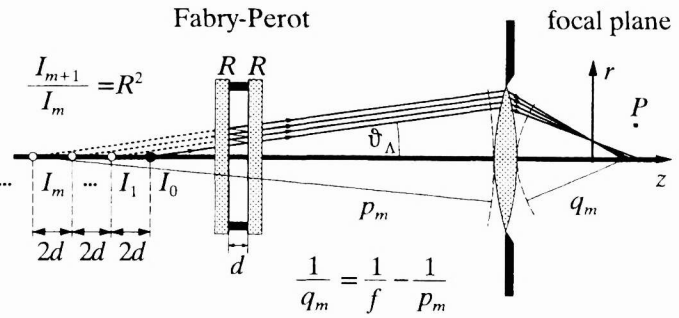

Fig. 2. Notations used for the calculations. The electric field is given by the sum of the fields generated by virtual sources I_0, I_1, ...

$$E(r,z) = -\frac{i k a^2 A_0}{2} \exp[i(kz + \Phi_0)] \sum_{m=0}^{\infty} \frac{[R \exp(i\delta)]^m}{p_m q_m} \left(C(u_m, v_m) - i S(u_m, v_m) \right) , \tag{2}$$

where r and z are the cylindrical coordinates of point P, k is the wave number, a is the radius of the lens aperture and Φ_0 is an unimportant phase factor. C and S functions can be calculated by the Lommel functions [15] and $u_m = k \cdot (a/q_m)^2 \cdot (f + z - q_m)$ and $v_m = k \cdot (a/q_m) \cdot r$ are dimensionless variables. Fig. 3 shows the intensity distribution of the field produced by a virtual source in the vicinity of the image point. In Eq. (2) δ is the phase difference between two neighboring virtual sources. If Λ denotes the greatest integral value which is less than or equal to $2d/\lambda$ then

$$\delta = \frac{4(d - d_0)}{\lambda} \pi = K\pi \quad , \tag{3}$$

where $d_0 = \Lambda \cdot \lambda/2$ and $K = 4(d - d_0)/\lambda$ (so $0 < K \leq 2$). A variation of d of $\lambda/2$ leads to a change of the phase difference of 2π. For such a small variation of d the position of image points of the virtual sources practically remains unchanged. Therefore δ and d can be regarded as independent variables.

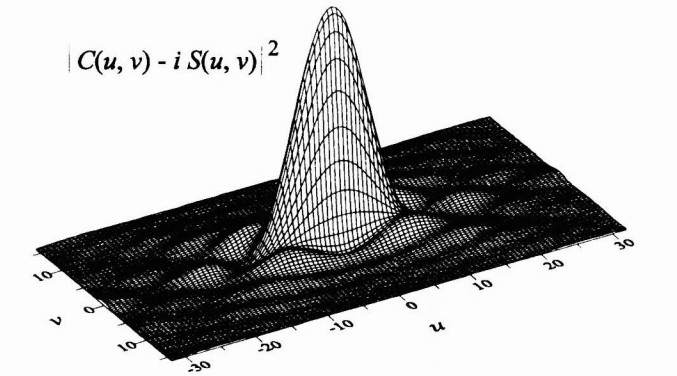

Fig. 3. $|C(u,v) - i S(u,v)|^2$ gives the intensity distribution of the focused field produced by a point source. In the image plane (u=0) it gives the well-known Airy–pattern given by $|2J_1(v)/v|^2$ and on the optical axis (v=0) it yields $|\sin(u/4)/(u/4)|^2$.

3. DISCUSSION

If the lens is illuminated by a point source the depth of focus [10] (Fig. 4)

$$DOF = \frac{2\lambda}{NA^2}(1+M)^2 \qquad (4)$$

is defined as the distance between the principal intensity maximum and the first intensity minimum on the optical axis, where $NA=a/f$ is the numerical aperture of the lens and M is the magnification. The distance between the image points of the virtual sources approximately equals to $2dM^2$. The relative image density defined by

$$N = \frac{DOF}{2dM^2} = \frac{\lambda}{d}\left(\frac{1+M}{NA\,M}\right)^2 \qquad (5)$$

is an important quantity to determine the shape of the axial intensity distribution [10]. During the experiment [10] four different cases were studied. The focal length and the numerical aperture of the lens used in the experiment were 50 mm and 1/11.2, respectively. The measured value of DOF was 220 μm. In this case from Eq. (4) the magnification M=0.1772 and the distance of the source I_0 from the lens is given by $p_0 = f\cdot(1+1/M) = 332.17$ mm. Fig. 5 shows the intensity distribution for various values of the image density N. The axial intensity distributions were fitted to the measured curves. The calculations have been done using Eq. (2) with the following parameters: (a) d=7431.6 μm (N=0.47), K=1.501 ; (b) d=3100 μm (N=1.13), K=0.35 ; (c) d=1091 μm (N=3.21), K=0.22 ; (c) d=436.6 μm (N=8.02), K=0.164 . The reflectivity R was assumed to be 0.963. These values of the parameters agree with their measured values within the accuracy of the measurement. The insets show the comparison of the measured (circles) and calculated (lines) intensity distribution on the optical axis. In case (a) the distance between the image points on the optical axis is large compared to the DOF. Thus sharp peaks can be seen separately. By increasing the image density (i.e. decreasing d) the oscillation on the optical axis disappears, the curves become smoother. The numbers adjacent to the peaks show the value of the peak intensity. In agreement with the law of conversation of the energy by increasing N the peak intensity increases.

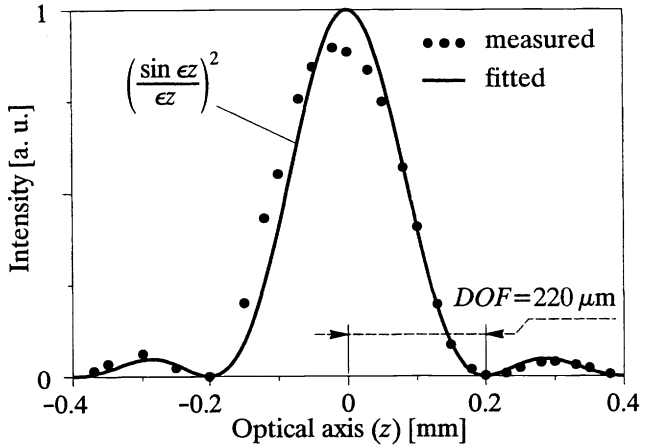

Fig. 4. The measured axial intensity distribution of a field produced by a point source in the vicinity of the image point.

Under certain circumstances the intensity distribution in a plane perpendicular to the optical axis can be described with the zero order Bessel function. The radius of the interference rings is different for different cases and slightly increases by increasing z as it can be seen in Fig. 6. The detailed analysis shows that the radius of the interference rings strongly depends on the phase difference δ. The intensity distribution (calculated from Eq. (2)) is plotted for various values of δ assuming N=2 (d=1751.6 μm). The values of coefficient K were 0.15 and 0.5 for cases (a)-(b), respectively. The insets in the top right corner show the intensity immediately in front of the lens. The insets in the top left corner show the radial intensity distribution in a plane given by z. The lines indicate the radial intensity distribution calculated from Eq. (2) and the circles display the result of Eq(6) (approximate analytical expression). By increasing δ the radius of the ring increases therefore the interference rings shrink in a plane perpendicular to the axis (see Fig. 6). Then the radial intensity distribution can approximately be described with [14]

$$I_B(r) = I_{B0}\,J_0^2\left(\frac{2\pi}{\lambda}\frac{l_B}{z}r\right), \qquad \text{where } l_B = f\sqrt{\left(\frac{K}{2\Lambda}+1\right)^2 - 1} = f\tan\vartheta_\Lambda \qquad (6)$$

and I_{B0} is the intensity on the axis at point z. Eq. (6) was plotted with circles in the insets of Fig. 6. The radial intensity distribution can be explained with a simple model. The Fabry-Perot interferometer transmits the light in directions ϑ_m given

by $\cos\vartheta_m = m/(2d/\lambda)$ where m is an integer between 1 and $2d/\lambda$. The integral value of Λ corresponds to the smallest angle ϑ_Λ. The light incident on the lens in direction ϑ_Λ is collected by the lens to a bright interference fringe in the focal plane (Fig. 2). The radius of the fringe is given by $l_B = f \tan\vartheta_\Lambda$. Using $\tan^2\vartheta_\Lambda = 1/\cos^2\vartheta_\Lambda - 1$ and the definition of K one can obtain Eq. (6) for l_B . Only one fringe is formed in the focal plane because the lens aperture is adjusted so that it transmits the first Fabry-Perot ring only and blocks all the others. So the observer at point z sees that the light arrives from a bright narrow ring lying in the focal plane. The radial intensity distribution of the diffraction pattern of a narrow ring can be described by Eq. (6). By increasing δ further the ring slips from the lens aperture and the intensity in front of the lens falls considerably. The illumination of the lens is similar to homogeneous illumination therefore the intensity distribution resembles the three dimensional Airy-pattern (Fig. 3).

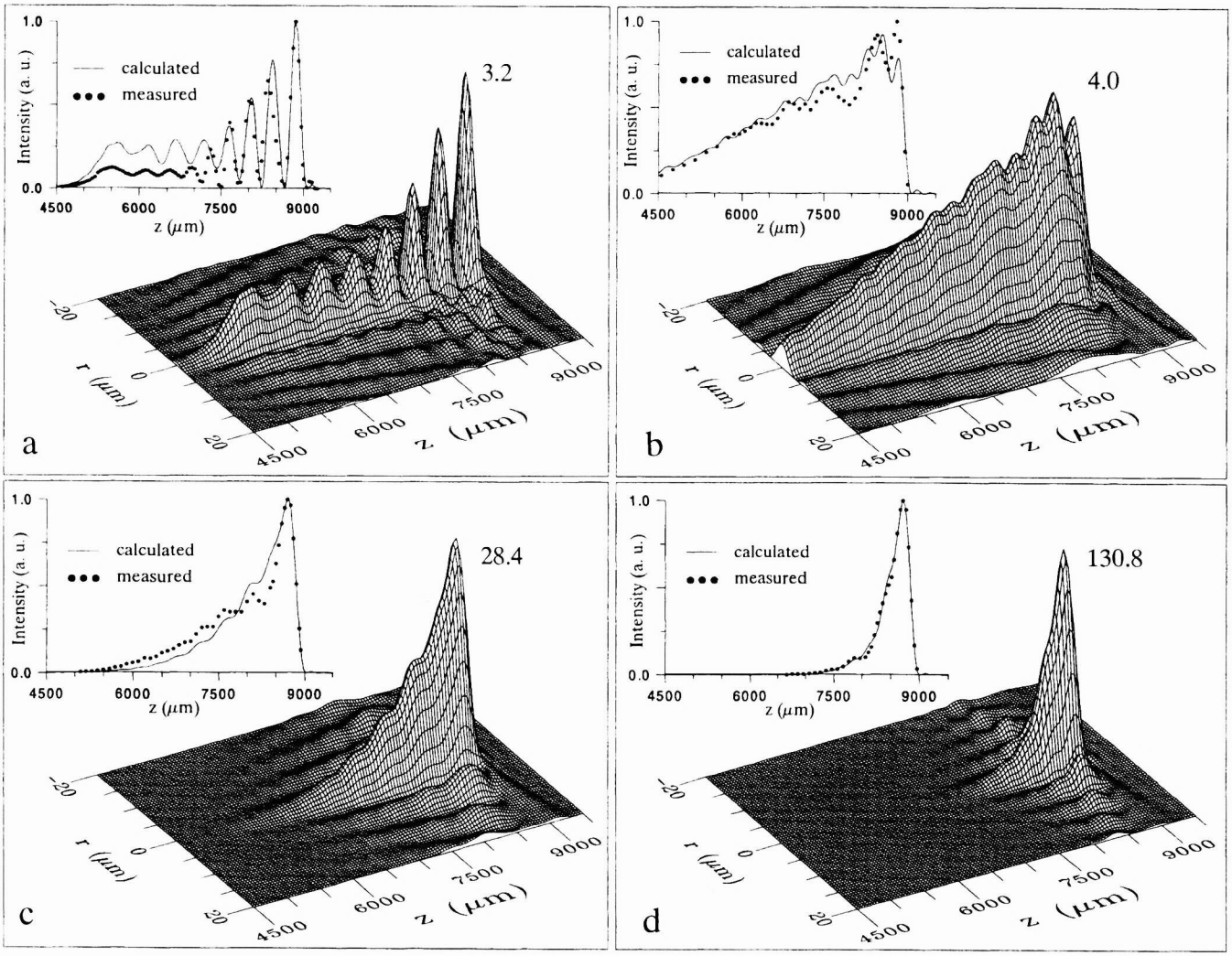

Fig. 5. The spatial intensity distribution (calculated from Eq. (2)) for different values of image density N and phase difference δ. The insets show a comparison of the calculated and measured axial intensity distribution.

4. CONCLUSIONS

A novel concept for generating nondiffracting Bessel beam has been studied theoretically. The spatial intensity distribution has been calculated with a wave optical model for various values of the image density and phase difference. An approximate analytical formula has been derived to describe the radial intensity distribution in planes perpendicular to the optical axis.

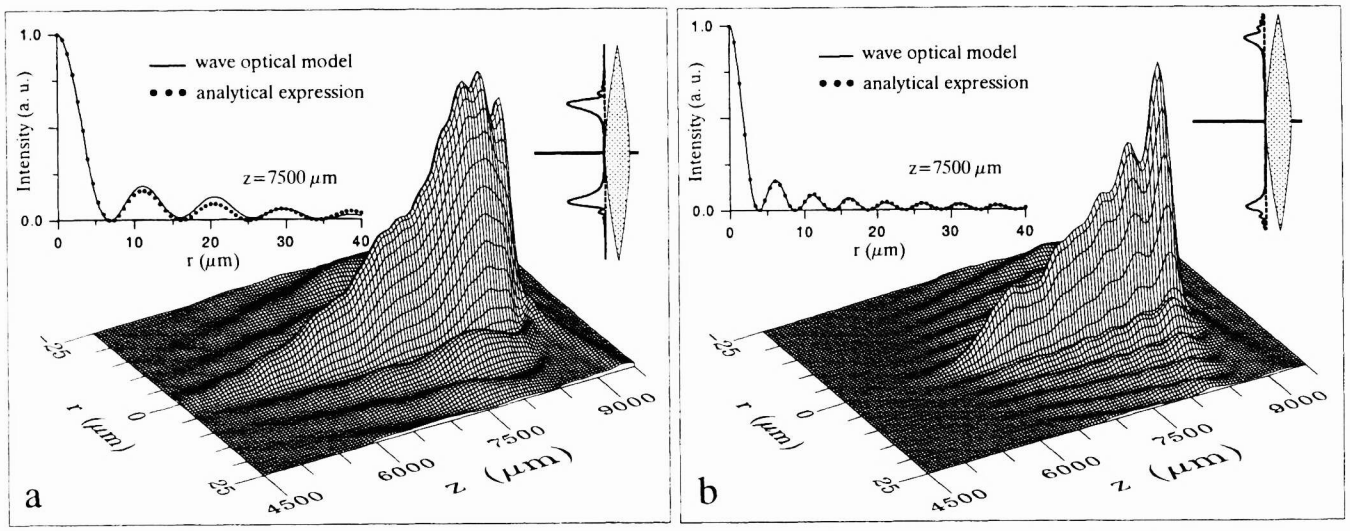

Fig. 6. The intensity distribution for different phase difference δ (assuming approximately constant image density N=2). The insets show the illumination of the lens (right) and a comparison of the radial intensity distribution calculated from Eq. (2) and Eq. (6) (left).

5. ACKNOWLEDGEMENT

This work was supported in part by Texas Instruments, NSF under grants DMI-9209639 and INT-9020541, and by the OTKA Foundation of the Hungarian Academy of Sciences (No: T20910 and F020889)

6. REFERENCES

1. J. Durnin, "Exact solution for nondiffracting beams. I. The scalar theory", *J. Opt. Soc. Am.* **4**, 651 (1987)
2. J. Durnin, J. J. Miceli, Jr. and J. H. Eberly, "Diffraction-free beams", *Phys. Rev. Lett.* **58**, 1499 (1987)
3. R. Arimoto, C. Saloma, T. Tanaka and S. Kawata, "Imaging properties of axicons in a scanning optical system" *Appl. Opt.* **31**, 6653 (1992)
4. J. Turunen, A. Vasara and A. T. Friberg, "Holographic generation of diffraction-free beams", *Appl. Opt.* **27**, 3959 (1988)
5. A. J. Cox and D. C. Dibble, "Holographic reproduction of a diffraction-free beam", *Appl. Opt.* **30**, 1330 (1991)
6. A. J. Cox and D. C. Dibble, "Nondiffracting beams from a spatially filtered Fabry-Perot resonator", *J. Opt. Soc. Am.* **9**, 282 (1992)
7. G. Indebetouw, "Nondiffracting optical fields: Some remarks on their analysis and synthesis", *J. Opt. Soc. Am.* **6**, 150 (1989)
8. J. K. Jabczynsky, "A 'diffraction-free' resonator", *Opt. Commun.* **77**, 292 (1990)
9. K. Uehara and H. Kikuchi, "Generation of nearly diffraction-free laser beams", *Appl. Phys. B* **48**, 125 (1989)
10. M. Erdélyi, Z. L. Horváth, G. Szabó, Zs. Bor, F. K. Tittel, J. R. Cavallaro and M. C. Smayling, "Generation of diffraction-free beams for application in optical microlithography", *J. Vac. Sci. Technol. B* **15**(2), 287 (1997)
11. G. B. Airy, "On the diffraction of an annular aperture", *Philos. Mag.* **18**, January 1841
12. E. H. Linfoot and E. Wolf, "Diffraction images in systems with annular aperture", *Proc. Phys. Soc.* **B66**, 145 (1953)
13. C. A. Taylor and B. J. Thompson, "Attempt to investigate experimentally the intensity distribution near the focus in error-free diffraction patterns of circular and annular apertures", *J. Opt. Soc. Am.* **48**, 844 (1958)
14. Z. L. Horváth, M. Erdélyi, G. Szabó, Zs. Bor, F. K. Tittel and J. R. Cavallaro, "Generation of nearly nondiffracting Bessel beams with Fabry–Perot interferometer", accepted in *J. Opt. Soc. Am. A.*
15. M. Born and E. Wolf, *Principles of optics*, sixth (corrected) edition (Pergamen Press, Oxford, 1989), ch. 8.8